



13TH CANADIAN MASONRY SYMPOSIUM
HALIFAX, CANADA
JUNE 4TH – JUNE 7TH 2017



REALISTIC WIND LOADS ON REINFORCED MASONRY WALLS

Tissera, Nipun¹ and Sparling, Bruce²

ABSTRACT

Wind is a primary source of out-of-plane loads for masonry wall structural members. Although wind is a dynamic load condition, the current body of research generally considers the behaviour of masonry walls under quasi-static load conditions, whilst the dynamic aspect is not explicitly considered. Therefore, this research intends to address this gap in knowledge. The objective of this research was to investigate the behavioural characteristics of reinforced masonry walls subjected to realistic wind load conditions. Specifically, the intention was to examine the differences in strength and ductility of reinforced masonry walls under quasi-static and dynamic load conditions. In addition, differences in the behaviour of walls with different levels of reinforcement were examined under quasi-static and dynamic load conditions. The experimental program consisted of testing twenty large scale wall specimens featuring ideal-pinned support conditions. The specimens comprised four sets of tests that addressed all possible combinations of the two primary test variables: quasi-static vs. dynamic load, and low vs. high reinforcement ratio. The partially grouted wall specimens had nominal dimensions of 3 m high and 1 m wide, and were constructed using standard 200 mm hollow concrete masonry blocks arranged in a running bond pattern. The dynamic load was generated using a 4th order autoregressive function to produce a series of realistic wind load time histories for varying wind intensities. The dynamic loads and the quasi-static loads were applied using a four-point loading setup. Both the strength and deformation characteristics of the wall specimens were analyzed and compared. The results indicate that the dynamically loaded walls resist somewhat higher peak loads and at higher levels of ductility.

KEYWORDS: *dynamic, masonry, reinforced, wall, wind*

¹ Masters Student Candidate, Department of Civil & Geological Engineering, University of Saskatchewan, 57 Campus Drive, Saskatoon, SK, Canada, tissera.n@usask.ca

² Professor, Department of Civil & Geological Engineering, University of Saskatchewan, 57 Campus Drive, Saskatoon, SK, Canada, bruce.sparling@usask.ca

INTRODUCTION

The general parameters of this study were based on a previous study which investigated the behaviour of unreinforced masonry walls under realistic wind load conditions. That study indicated that the unreinforced masonry walls exhibited slightly higher capacity under dynamic wind load conditions, particularly when realistic support conditions were considered [1]. Overall, though, research regarding out-of-plane behaviour of masonry walls under dynamic loads is limited and mostly related to either earthquake or blast-induced loading. Response to wind-like loads has generally been considered under quasi-static conditions where the dynamic aspect has not been explicitly considered.

Wind exerts a random pressure loading, which varies both spatially and over time. It consists of a steady mean component and a dynamic gust component which fluctuates randomly about the mean pressure. Current design standards characterize wind load as static pressure defined at a specified mean wind speed, which is magnified by a “gust factor” to account for the peak loads produced by the dynamic fluctuations [2]. Therefore, the structure is assumed to behave in a quasi-static manner at ultimate conditions, without explicitly considering dynamic effects.

OBJECTIVE

The objective of this research was to investigate the behaviour of reinforced masonry walls subjected to realistic out-of-plane wind loading. Specifically, the research was intended to:

- Compare the load resisting and displacement characteristics under quasi-static loads representative of a steady uniform wind pressure and dynamic loads representative of a realistic wind storm; and
- Examine the behavioural characteristics of reinforced masonry walls, with ideal pinned support conditions, at different levels of steel reinforcement under both quasi-static and dynamic loading conditions.

EXPERIMENTAL PROGRAM

The experimental program was carried out in two phases. Phase one comprised the construction and testing of the low reinforcement ratio specimens, while phase two comprised the construction and testing of the high reinforcement ratio specimens. Twenty large scale wall specimens were constructed and tested under ideal-pinned support conditions. The specimens were divided into four sets, each consisting of five replicated specimens, which addressed all possible combinations of the two primary test variables: quasi-static vs dynamic wind load conditions and low vs high reinforcement ratios. The four sets were:

- Specimens with a low reinforcement ratio tested under quasi-static loads (denoted by LS);
- Specimens with a low reinforcement ratio tested under dynamic loads (denoted by LD);
- Specimens with a high reinforcement ratio tested under quasi-static loads (denoted by HS); &
- Specimens with a high reinforcement ratio tested under dynamic loads (denoted by HD)

The wall specimens were 15 courses high and 2.5 blocks wide. They were constructed in a running bond pattern using standard 200 mm hollow concrete blocks with nominal compressive strength of 15 MPa. Type S mortar cement mix was used and the walls had face-shell mortar bedding with concavely tooled 10 mm mortar joints. Therefore, the nominal dimensions of the specimens were approximately 3000 x 1000 x 190 mm. The wall specimens were designed to be under-reinforced as per provisions provided in CSA S304.1-14 [3]. The specimens with low and high reinforcement ratios were provided with one 10M and one 15M bars, respectively, at mid-depth of the 2nd and 4th cells from the ends of the walls. The walls were partially grouted with only the cells in which the bars were placed being grouted.



Figure 1: Test Setup (left) and Instrumentation (right)

Figure 1 shows the four-point loading setup that was used to approximate the uniformly distributed wind load conditions. Both types of loads were applied using a horizontally oriented hydraulic actuator positioned at the mid-height of the wall specimens. Two equal line loads, which were 800 mm apart at 1100 mm and 1900 mm, respectively, above the support level, were applied using a spreader system.

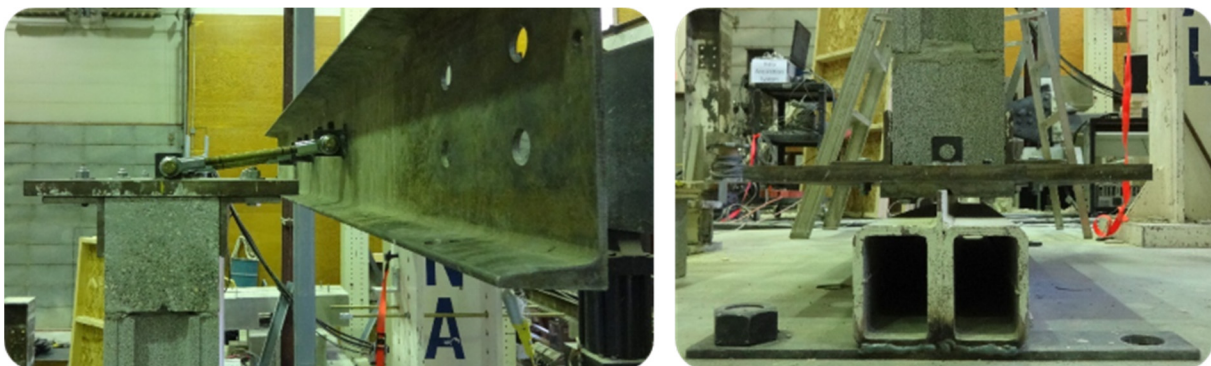


Figure 2: Top (left) and Bottom (right) Support Configurations

The wall specimens were tested under ideal-pinned support conditions. Figure 2 shows the top and bottom support configurations. The top support was such that horizontal motion was restricted while allowing limited vertical motion and joint rotation. The bottom knife-edge support restricted both horizontal and vertical motion while allowing joint rotation. Full width steel angles bolted to the steel plates prevented sliding of the wall specimens under load.

An MTS[®] Series 244 hydraulic actuator featuring a built-in force transducer and linearly variable differential transducer (LVDT) was used to apply the loading. The mid-height deflection was measured using a Micro-Epsilon optoNCDT 1700-500 laser optical displacement measurement device. A secondary pair of load cells and LVDTs were also used to measure loads applied by each spreader arm and to measure deflections along the wall height. The data was sampled at a rate of 100 Hz and was recorded using LabView[®] software suite for further processing.

The quasi-static loads were applied under displacement control at a rate of 6 mm/s. The dynamic loads were applied under load control as a series of load time histories with increasing intensity. Further details on dynamic loading is provided in the following section. In both cases, the specimens were loaded beyond the yield load and testing was halted once the deformation of the walls reached the feasible limits of the test setup. Additional testing was done in conjunction to correlate material and assemblage properties with the behaviour of the wall specimens.

WIND LOAD PROFILE GENERATION

Mathematical modelling was used to generate the wind profiles. They were generated using a 4th order autoregressive function, using a similar approach to that used in previous studies [4]. The general behaviour and frequency content of the generated wind histories were based on a theoretical power spectrum density (PSD) function for gusty winds, as proposed in the literature [5]. The wind speed time histories were generated for specific mean wind speeds, were 10 minutes in duration, and defined at 0.05 s intervals. The model assumed a reference height of 10 m above ground and a typical suburban terrain surrounding [6]. The profiles were converted to load time histories assuming the wall specimens had a nominal surface area of 3 m² and a drag coefficient of 1.0. An initialization period of 2 min was added to the beginning of the load time histories to avoid the application of a sudden impact at the start of a load profile. The load was gradually increased to the mean value after which the dynamic component was again increased gradually from zero to its full value.

However, it was uncertain in advance the degree to which a load time history would affect a wall specimen, given that it was based on a specific mean wind speed. Therefore, a series of load time histories with increasing intensity needed to be applied to a wall specimen until failure. The series was selected such that the intensity of the first load time history represented a mean wind speed of 30 m/s, which did no significant damage to the wall specimens. The intensity of the subsequent load time histories within a series was increased in 10 m/s increments until the limits of the test setup in loading the wall specimens were reached. The increment was chosen considering both the resolution of the gathered data and the time taken to complete testing of one

specimen. Thus, five unique series of load time histories were generated, with each series applied to a pair of wall specimens: one low reinforcement ratio specimen and one high reinforcement ratio specimen.

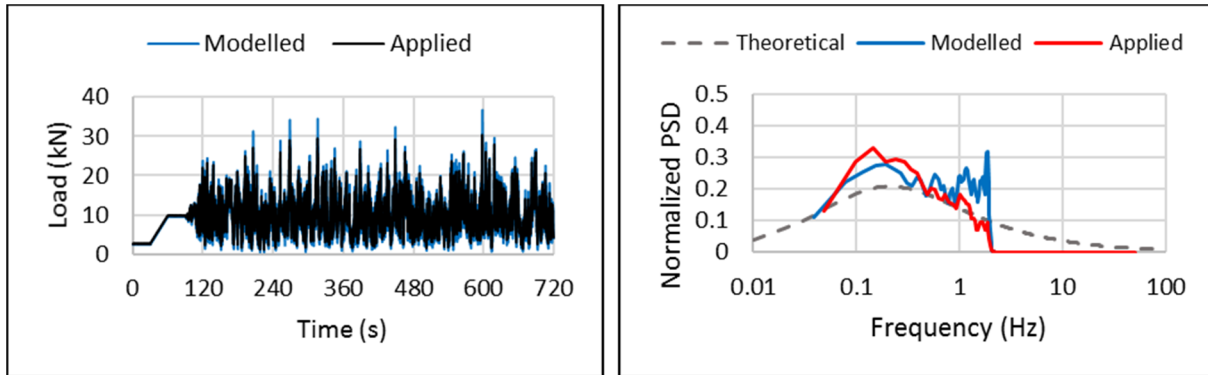


Figure 3: Load Time History (left) and PSD (right) Plots of HD2 for 70 m/s Wind Intensity

Figure 3 presents the load time history and the PSD plots of the 70 m/s intensity wind load applied to the 2nd dynamically loaded high reinforcement ratio specimen (HD2). The plots represent the total load modelled and applied by the actuator. The PSD plots were normalized using their respective root mean square values; the theoretical curve is based on gusty wind storms proposed in the literature. The plots indicate good agreement between the applied load and a realistic wind storm. However, as the Nyquist frequency of the generated time history was 2 Hz, the modelled and applied loads did not contain frequency content higher than this value. Furthermore, at higher load intensities, such as this where the specimens had incurred significant damage, their high deflection and compliance prevented the applied loads from reaching some of the peaks that were in the modelled profiles. In contrast, Figure 4 presents the plots of the same profile applied to the 2nd dynamically loaded low reinforcement ratio specimen (LD2). The plots indicate much poorer agreement with the realistic wind storm; this was due to limitations in the actuator control system, a condition that was rectified prior to the high reinforcement ratio tests. Thus, the dynamic loads applied to the low reinforcement specimens did not contain much of the high frequency content and corresponding peak loads expected in a realistic wind storm.

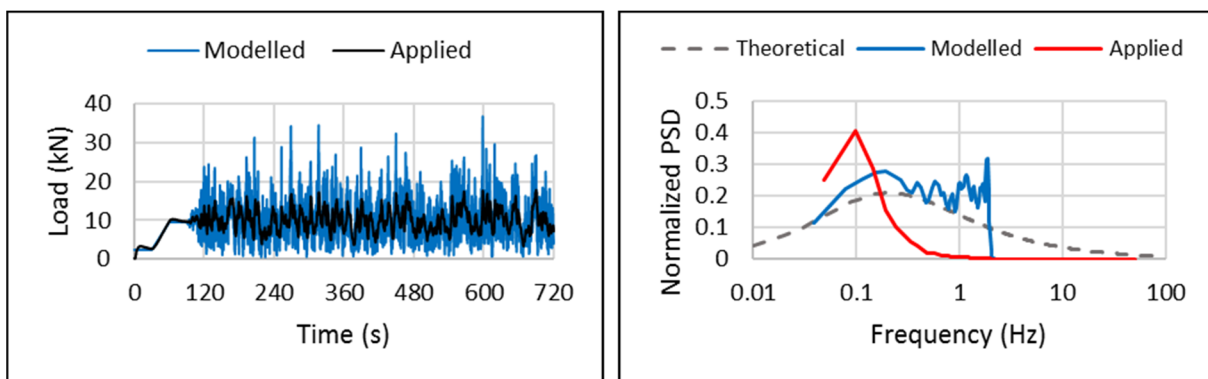


Figure 4: Load Time History (left) and PSD (right) Plots of LD2 for 70 m/s Wind Intensity

TEST RESULTS

Table 1 provides the mean values and the coefficient of variation (CV) of the material and assemblage properties of the wall specimens that were tested under both loading conditions. Although the prism strengths showed a slight difference between the low and high reinforcement ratio specimens, the specimens had similar material properties overall.

Table 1: Summary of Material and Prism Test Results

Reinforcement Ratio	Reinforcement Strength		Mortar Compressive Strength		Grout Compressive Strength		Prism Compressive Strength			
	Yield (MPa)	Ult. (MPa)	Mean (MPa)	CV (%)	Mean (MPa)	CV (%)	UngROUTED		ROUTED	
							Mean (MPa)	CV (%)	Mean (MPa)	CV (%)
Low	440.74	665.55	19.62	24.49	22.37	14.00	14.33	8.03	11.48	10.57
High	436.83	659.24	20.65	12.71	20.52	11.17	12.08	7.53	9.98	13.24

Quasi-Static Test Results

Figure 5 presents the load vs deflection results of the specimens tested under quasi-static load conditions. The load presented is the total load applied by the actuator, while the deflection presented is the mid-height deflection of the wall specimens.

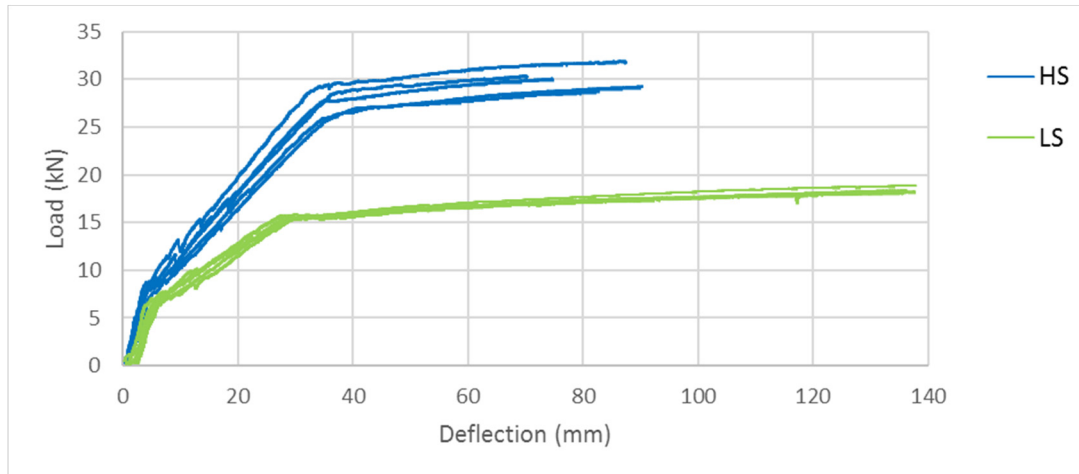


Figure 5: Load vs Deflection Plots of the Quasi-Static Loading Tests

The damage patterns for both LS and HS specimens were similar; in that they responded in a typical flexural ductile mode expected of reinforced masonry members [7]. The plots indicated the first distinct change in response at the onset of bed-joint cracks in the mid-height constant moment region. These cracks occurred at the block mortar interface over the entire width of the wall specimens. The cracking moment and deflection results provided in Table 2 refer to this point where there was a notable change in stiffness of the wall specimens. The moments presented are the values within the constant moment region, while the deflections presented are the corresponding mid-height deflections.

As the load resisted by the specimens increased, further bed-joint cracks propagated outward from the mid-height region. The plots indicated the next distinct change in response at the onset of significant plastic deformation. At this point the bed-joint cracks in the constant moment region widened significantly and the reinforcement yielded. The yielding results provided in Table 2 refer to this point where there was this second significant change in stiffness of the wall specimens. Beyond this point the rate at which the load increased was drastically reduced. The testing was halted once further support rotation and specimen deflection were no longer feasible for the test setup. The maximum applied results provided in Table 2 refer to this point. At the end of the tests there were significant bed-joint cracks in the mid-height region on the tension face, but no crushing or spalling evident on the compression face of the wall specimens.

Table 2: Moment and Deflection Results of the Quasi-Static Loading Tests

Specimen	Cracking		Yielding		Maximum Applied		
	Moment (kNm)	Deflection (mm)	Moment (kNm)	Deflection (mm)	Moment (kNm)	Deflection (mm)	
Low Reinforcement Ratio	LS1	3.65	4.20	8.94	28.20	10.46	132.08
	LS2	3.57	5.74	8.82	30.00	10.44	137.74
	LS3	3.85	5.80	8.70	27.92	10.41	132.08
	LS4	3.71	6.28	8.91	29.33	10.53	136.20
	LS5	3.75	5.24	9.01	27.53	10.81	137.89
High Reinforcement Ratio	HS1	4.26	3.77	15.94	35.49	17.22	74.86
	HS2	4.72	4.62	14.85	35.18	16.50	82.78
	HS3	4.87	4.55	16.31	36.91	17.40	70.38
	HS4	4.14	4.76	15.11	38.00	16.75	90.37
	HS5	4.99	4.09	16.75	34.29	18.28	87.49

Dynamic Test Results

The damage patterns of the dynamically loaded specimens, LD and HD specimens, were comparable to that of the specimens tested under quasi-static loading. Therefore, the two distinct changes in responses at the onset of cracking and at the onset of significant plastic deformation were likewise observed in the dynamic test results. However, a different set of criteria needed to be followed when determining load and deflection values of these damage states under dynamic testing, compared to that of quasi-static testing. This was because specimens under dynamic load conditions were subjected to a series of wind load profiles with increasing intensities. Initially, the intensity of the wind load profiles at which these damage states occurred were determined through visual observation. The deflection time histories were then analysed for significant changes in the mean deflection. The corresponding instance of the peak loads which resulted in these changes were determined from the applied load time histories, as these damage states occurred. Furthermore, the load-deflection hysteresis diagrams were analysed to confirm the load and deflection at which these distinct changes in the wall specimen stiffness occurred.

The general behaviour of both LD and HD specimens were consistent throughout the wind load profiles of each intensity. At the lowest intensity load profiles of 30 m/s mean wind speed, the specimens did not sustain any significant damage. Both LD and HD specimens began developing cracks at 40 m/s intensity load profiles. As an example, Figure 6 presents the deflection time history and hysteresis plots of the 40 m/s intensity wind load applied to the specimen HD5. The deflection time history shows a significant change in mean deflection at approximately 400 s where the first cracks appeared in this specimen. Correspondingly, the hysteresis diagram shows a notable change in wall stiffness. Note that the load presented is the total load applied by the actuator and the deflection presented is the mid-height deflection of the wall specimens.

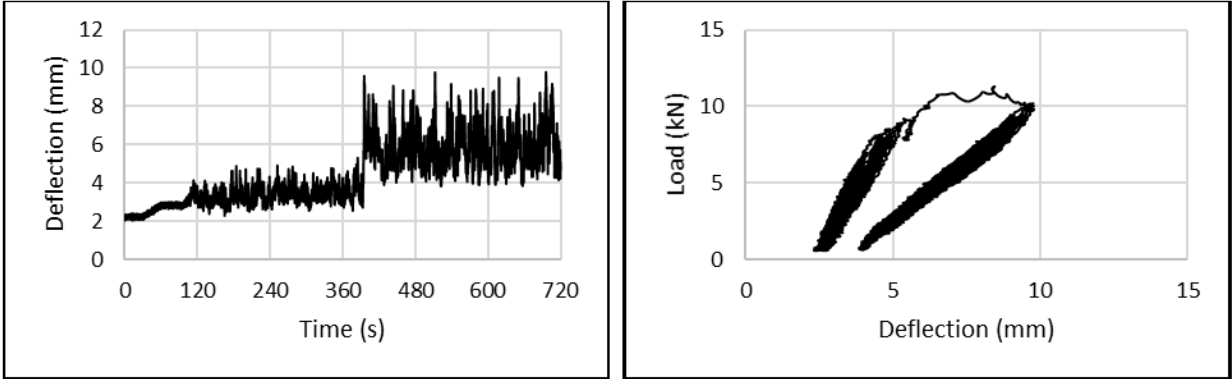


Figure 6: Deflection Time History (left) and Load-Deflection Hysteresis (right) Plots of HD5 for 40 m/s Wind Intensity

At the 50 m/s and 60 m/s intensity load profiles, the wall specimens sustained gradual damage, but did not exhibit significant plastic deformation until the 70 m/s intensity load profiles were applied. As an example, Figure 7 presents the deflection time history and hysteresis plots of the 70 m/s intensity wind load applied to the specimen HD2. The deflection time history shows a significant change in mean deflection at approximately 250 s. The corresponding instance where plastic deformation begins is also evident in the hysteresis diagram.

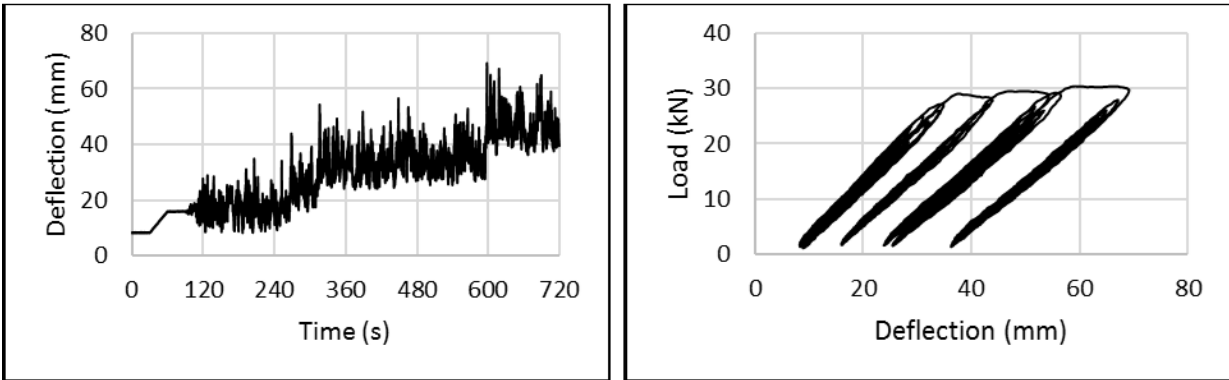


Figure 7: Deflection Time History (left) and Load-Deflection Hysteresis (right) Plots of HD2 for 70 m/s Wind Intensity

At the 70 m/s mean wind speed load profiles, the feasible limits of the test setup were reached and higher intensity load profiles were not possible due to the large plastic deformation of the wall specimens. The specimens had significant bed-joint cracks in the mid-height region on the tension face, but no crushing or spalling on the compression face at the completion of testing. Table 3 provides the moment values in the constant moment region and the mid-height deflections of the dynamically loaded wall specimens at the two damage states discussed in the above sections: cracking and yielding. The maximum applied values refer to the maximum moment and deflection which resulted from the highest intensity wind load profile applied to each wall specimen.

Table 3: Moment and Deflection Results of the Dynamic Loading Tests

Specimen	Cracking		Yielding		Maximum Applied		
	Moment (kNm)	Deflection (mm)	Moment (kNm)	Deflection (mm)	Moment (kNm)	Deflection (mm)	
Low Reinforcement Ratio	LD1	3.77	3.70	9.05	32.85	10.36	123.39
	LD2	3.68	3.96	9.16	34.33	10.18	90.82
	LD3	3.65	6.46	9.19	35.88	10.64	141.75
	LD4	4.16	11.08	9.05	35.64	10.67	136.52
	LD5	3.49	4.22	9.16	31.45	10.64	110.92
High Reinforcement Ratio	HD1	4.37	7.60	15.49	43.47	16.64	101.73
	HD2	4.49	5.80	16.60	37.87	17.38	69.17
	HD3	4.71	7.34	17.38	37.81	18.26	64.37
	HD4	4.51	6.06	16.34	38.50	17.79	82.17
	HD5	5.12	5.42	16.92	39.40	17.09	47.41

Summary

Table 4 provides the mean values and the coefficient of variation (CV) of the moment and the mid-height deflection at cracking and yielding damage states of all four sets of reinforced masonry wall specimens that were tested under quasi-static and realistic dynamic wind load conditions.

Table 4: Summary of Moment and Deflection Results

Specimens		Mean Cracking				Mean Yielding			
Reinforcement Ratio	Loading Type	Moment (kNm)	CV (%)	Deflection (mm)	CV (%)	Moment (kNm)	CV (%)	Deflection (mm)	CV (%)
Low	Static	3.71	2.82	5.45	14.53	8.88	1.37	28.60	3.62
	Dynamic	3.75	6.71	5.88	52.81	9.12	0.75	34.03	5.52
High	Static	4.60	8.25	4.36	9.52	15.79	5.07	35.97	4.10
	Dynamic	4.64	6.34	6.44	15.04	16.54	4.26	39.41	5.99

Figure 8 summarises the strength results of the wall specimens at specific damage states. There was insufficient evidence to make statistically significant conclusions. However, both low and high reinforcement ratio specimens indicated a slight increase in the yield capacity under realistic dynamic wind load conditions: a 3% and a 5% increase, respectively. The load at the first appearance of cracks did not indicate any difference in capacity under the two types of loading.

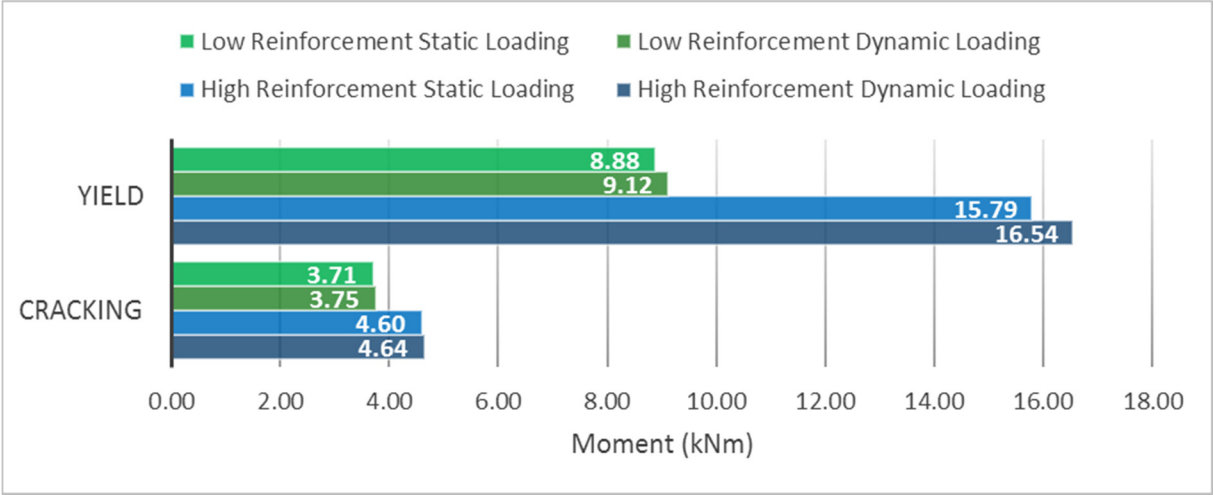


Figure 8: Summary of Moment Results at Cracking and Yielding Conditions

Figure 9 summarises the mid-height deflection results of the wall specimens at specific damage states. There was sufficient evidence to indicate a statistically significant difference in deflection at yielding between the two types of loading. The low and high reinforcement specimens indicated an increase of 20% and 10%, respectively, under realistic dynamic wind load conditions. However, there was insufficient evidence to indicate a statistically significant difference in deflection at cracking between the two types of loading.

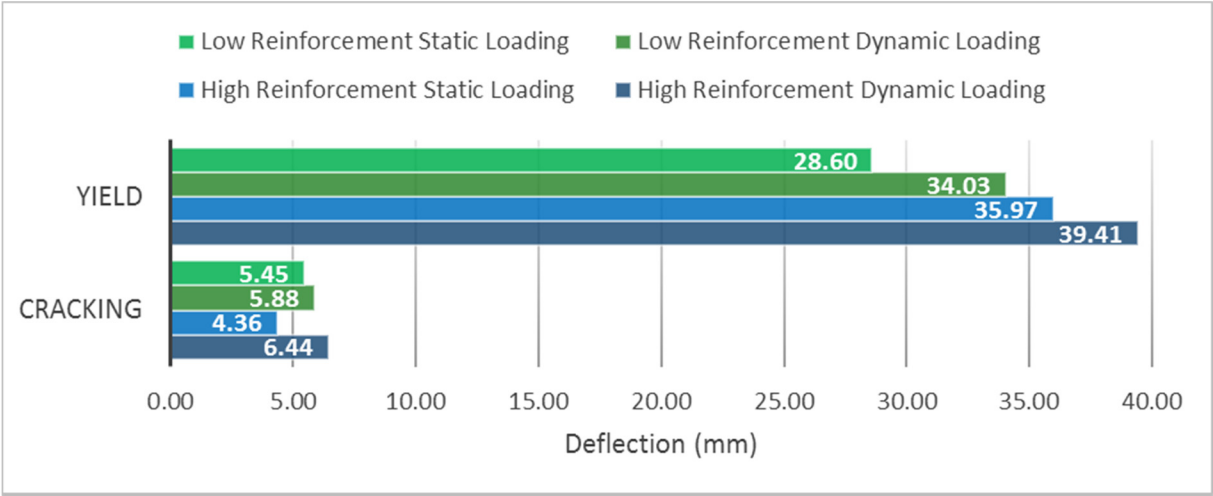


Figure 9: Summary of Deflection Results at Cracking and Yielding Conditions

DISCUSSION

The results indicate that reinforced masonry walls resist somewhat higher peak loads and higher levels of ductility under realistic wind loading, as compared to those for quasi-static loading. However, there does not seem to be such a difference at loads where the first cracks appear. This may have been due to the different mechanisms involved in the two damage states. The mechanism at yielding may be influenced by the rate of loading of the reinforcing steel, whereas cracking involves the loss of bond between the mortar and concrete block surface.

Furthermore, the high reinforcement ratio walls indicate a higher difference in yield load under the two types of loading than the low reinforcement ratio walls. This may have been due to the difference in the level of reinforcement. On the other hand, due to previously mentioned problems with the load controller, the dynamic load applied to the lower reinforcement ratio walls featured less high frequency content as compared that applied to the higher reinforcement ratio walls, which may also have contributed to this difference. Overall, though, the walls exhibited behaviour that was broadly similar to that observed under quasi-static loading.

ACKNOWLEDGEMENTS

The study was made possible by the funding provided by the Saskatchewan Masonry Institute and the University of Saskatchewan College of Engineering. The authors would like to thank the laboratory technician, Brennan Pokoyoway, and fellow colleagues in the graduate program at University of Saskatchewan for all the assistance, as well as Roy Nicholas from Gracom Masonry Ltd. who carried out construction of the specimens.

REFERENCES

- [1] Udey, A. (2014). *Realistic Wind Loads on Unreinforced Masonry Walls*. (M.Sc.), University of Saskatchewan, Saskatoon, SK, Canada.
- [2] NRC. (2010). National Building Code of Canada, National Research Council of Canada, Ottawa, Canada.
- [3] CSA. (2014). Design of masonry structures. CSA Standard S304.1-14, Canadian Standards Association, Mississauga, ON, Canada.
- [4] Sparling, B.F., and Davenport, A.G. (1998). "Three-dimensional dynamic response of guyed towers to wind turbulence." *Can. J. of Civil Eng.*, 25:512-525.
- [5] Kaimal, J.C., Wyngaard, J.C., Izumi, Y., and Coté, O.R. (1972). "Spectral characteristics of surface-layer turbulence." *Quarterly J. of the Royal Meteorological Society*, 98: 563-589.
- [6] Simiu, E., and Scanlan, R.H. (1987). *Wind Effects on Structures*, John Wiley & Sons, Inc., Hoboken, N.J. USA.
- [7] Abboud, B. E., Hamid, A. A., & Harris, H. G. (1996). Flexural behavior of reinforced concrete masonry walls under out-of-plane monotonic loads. *ACI Str. J.*, 93(3), 327-335.